22.5 A Bio-Impedance Readout IC with Digital-Assisted Baseline Cancellation for 2-Electrode Measurement

Hyunsoo Ha[1], Wim Sijbers[2], Roland van Wegberg[1], Jiawei Xu[1], Mario Konijnenburg[1], Peter Vis[1], Arjan Breeschoten[1], Shuang Song[2], Chris Van Hoof[2,3], Nick Van Helleputte[2]

[1]imec - Netherlands, Eindhoven, The Netherlands
[2]imec, Heverlee, Belgium
[3]KU Leuven, Heverlee, Belgium

Recent advances in wearables allow for monitoring the health status of users without disturbing their daily lives (Fig. 22.5.1). Bio-Impedance (BIOZ) is an interesting sensing modality for impedance cardiography, respiration measurement, and body composition analysis [1-4]. However, existing solutions rely on a 4-electrode measurement, where two leads are used for the current generator (CG), and the others for the readout front-end (RFE). This eliminates the effect of the electrode-tissue impedance (ETI) and measures the actual BIOZ, which is required in body composition analysis where the absolute value is important. However, this degrades user comfort and adds to system complexity and cost. This work proposes a BIOZ readout IC supporting 2-electrode BIOZ measurement of body signals, where relative changes over time yields the desired information (heartrate, respiration, etc.), with a good accuracy as a 4-electrode setup (Fig. 22.5.1). The ASIC can even measure the heartrate at the wrist via 2 electrodes, which consumes significant less power than the Photoplethysmography.

In the 2-electrode setup, the increased baseline impedance (>500Ω) due to the ETI ($2\times Z_{ELEC}$) imposes new challenges (Fig. 22.5.1). First, the RFE should achieve a wide input range with a high Signal-to-Noise Ratio (SNR) to detect small variations of BIOZ (0.1 to 10Ω) over the large baseline. A Current-Balancing Instrumentation Amplifier (CBIA) is widely used for competitive performance (power efficiency, low-noise, etc.) [2-4]. However, CBIAs exhibit input-amplitude-dependent noise behavior, resulting in unacceptable high noise and limited SNR in the presence of a large input amplitude [5], which is the case in a 2-electrode setup. Second, current noise from the CG appears as voltage noise at the input of the RFE and is further amplified by the Z_{ELEC}. Hence it is even more important to minimize the current noise of the CG. While Dynamic Element Matching (DEM) can mitigate the flicker noise component of the CG noise ($i_{N.CG}$) significantly [2], the noise ($i_{N.REF}$) contribution of the reference current (I_{REF}) remains unaddressed. Consuming more power and adopting chopper stabilization are conventional ways to mitigate thermal and 1/f noise in $i_{N.REF}$; however, they increase power and design complexity. In this paper, we propose digital-assisted baseline impedance cancellation to mitigate the RFE noise dependency on the (large) input amplitude (impedance). Additionally, an I_{REF} correlated noise-cancelling architecture is introduced to reduce the CG's noise contribution without utilizing low-noise current references.

Figure 22.5.2 shows the block diagram of the IC, which contains a CBIA including transconductance (TC), transimpedance (TI) stages, and baseline-cancellation current DAC (IDAC) and current-generating circuitry including the CG and IDAC which share I_{REF}. The RFE is designed to obtain in- (I) and quadrature-phase (Q) BIOZ simultaneously, and a pre-demodulation is adopted to reduce CBIA power [2,4]. In the CBIA, the signal-dependent current flows to the current mirrors between the TC-TI stages (T1 and T2 in Fig. 22.5.2) and hence 1/f noise is also input-signal dependent. This nonlinear effect results in noticeable 1/f noise in the presence of a large input despite chopping [5]. We propose a baseline cancellation loop comprising a digital controller and a fully differential IDAC (Fig. 22.5.3) which effectively acts as a DC servo. The large baseline current (I_{BASE}) is subtracted from the signal current (I_{TC}) directly in the TC such that the TC-TI current mirrors only see a residual current (I_{TC}-I_{BASE}) effectively reducing the nonlinear effect and the associated 1/f noise in the presence of a large input (Fig. 22.5.3). The input and the cancellation current are modulated by an identical clock (f_{chop}) for synchronization. The digital controller monitors the output of the I-channel and determines the I_{BASE} (0 to 11.75μA in 250nA steps) that satisfies the required threshold $|I_{TC}$-$I_{BASE}|$<150nA to ensure negligible noise modulation (Figs. 22.5.2 and 22.5.3). Since the baseline is derived in the digital domain, the complete full-scale impedance can be reconstructed, which cannot be done with an analog DC servo loop [3]. This is useful for checking the contact status in the 2- and 4-electrode scenarios with a large body impedance (>100Ω).

Figure 22.5.3 compares the measured noise performance with and without baseline cancellation. All noise numbers are measured by applying a current to a known resistor and taking the digital output to include all noise sources (CG, RFE, IDAC and ADC). A noise density at 1Hz and an integrated noise (0.1 to 4Hz) have been reduced from 310 to 98nV/√Hz and 619 to 198nV_{RMS}, respectively (with the largest input for the conventional CBIA (25mV_{PK})). Furthermore, since the large baseline is subtracted in the first TC stage, the CBIA can be configured to the largest gain (160V/V) relaxing the ADC noise requirement over the whole extended input range (<125mV_{PK}). In the conventional case [2], the IA gain must be reduced to accommodate a large input resulting in noise fluctuation when gain changes (Fig. 22.5.3).

The noise contribution of the IDAC also matters. The total BIOZ noise is the sum of all uncorrelated noise powers of the building blocks. In this work, DEM is also adopted in the IDAC, hence most of the uncorrelated noises (1/f noise) of the CG and the IDAC are mitigated. It is noteworthy that since both the CG and the IDAC use the same reference current, the remaining noise (in I_{BASE}, I_{CG} and I_{TC}) are largely correlated (amplified noise of $i_{N.REF}$ as in Fig. 22.5.4). Therefore, since the circuit cancels most of the I_{TC} by subtracting I_{BASE}, the correlated reference noise is also cancelled in TI ($i_{N.TI}$) due to the identical amplification ratio of signal and noise: I_{REF} to I_{TC} and I_{BASE} are equal to $i_{N.REF}$ to $i_{N.TC}$ and $i_{N.BASE}$ (Fig. 22.5.4). The maximum $|I_{TC}$-$I_{BASE}|$ of 150nA is small enough to make the residual $i_{N.REF}$ negligible for BGR noise <10μV/√Hz, which is achievable in low power (<5μW) without chopping. The correlated noise cancellation reduces the noise dramatically in comparison to the noise with uncorrelated input signal (Fig. 22.5.4) (e.g., V_{IN}=125mV_{PK}, noise density at 1Hz and integrated noise (0.1 to 4Hz) is reduced from 1789 to 436nV/√Hz and 3441 to 869nV_{RMS}, respectively).

The IC is fabricated in 55nm CMOS and occupies 0.738mm^2 (Fig. 22.5.7). The IC consumes 18.9 to 34.9μW from the RFE (2-electrode case of BIOZ-I only, V_{IN}=0.1 to 125mV_{PK}) and 31.4 to 154.7μW from the CG (I_{CG}=5 to 100μA_{PK}) from a single 1.2V power supply. For the 4-electrode case where the I- and Q-channel are operating, the RFE consumes 39.1μW (V_{IN}=10mV_{PK}). The noise performance has been characterized over whole input range (V_{IN}=0.1 to 125mV_{PK} with Z_{LOAD}=20Ω to 24kΩ) in Fig. 22.5.5. The work achieves a wide input range of 24kΩ and a fine resolution of 0.8$m\Omega_{RMS}$ and 13.9$m\Omega_{RMS}$ for Z_{LOAD} of 20Ω and 2kΩ, respectively, resulting in a dynamic range of 141dB and a maximum SNR of 94dB. There are remaining noise dependencies to the input signal due to 1/f noise of the cascode transistors in CG and IDAC that are not mitigated by DEM and a thermal noise of CG and IDAC, which become non-negligible with large impedance. Nevertheless, the body signals are successfully measured with 2-electrode (gel) on chest and 2-electrode (dry) on wrist for respiration and heartbeat (an additional electrode was used for body bias), respectively. It demonstrates that the IC has the required sensitivity to detect very small variations of impedance (<100mΩ) over a large baseline, which has not previously been demonstrated at IC level (Fig. 22.5.5). Figure 22.5.6 benchmarks the proposed IC with the state of the art. The proposed work achieves the best power efficiency and the widest dynamic range among reported solutions by addressing 2 critical challenges with a single solution.

References:

[1] P. Schönle, et al., "A Multi-Sensor and Parallel Processing SoC for Miniaturized Medical Instrumentation," *IEEE JSSC*, vol. 53, no. 7, pp. 2076-2087, July 2018
[2] H. Ha, et al., "A Bio-Impedance Readout IC with Frequency Sweeping from 1k-to-1MHz for Electrical Impedance Tomography," *Symp. VLSI Circuits,* pp. C174-C175, June 2017.
[3] M. Kim, et al., "A 1.4mΩ-Sensitivity 94dB-Dynamic-Range Electrical Impedance Tomography SoC and 48-Channel Hub SoC for 3D Lung Ventilation Monitoring System," *ISSCC Dig. Tech. Papers*, pp. 354-355, Feb. 2017.
[4] H. Ko, et al., "Ultra Low Power Bioimpedance IC with Intermediate Frequency Shifting Chopper," *IEEE TCAS-II*, vol. 63, no. 3, pp. 259-263, Mar. 2016.
[5] H. Ha, et al., "Measurement and Analysis of Input-Signal Dependent Flicker Noise Modulation in Chopper Stabilized Instrumentation Amplifier," *IEEE Solid-State Circuits Letters*, vol. 1, no. 4, pp. 90-93, Apr. 2018.

 978-1-5386-8531-0/19/$31.00

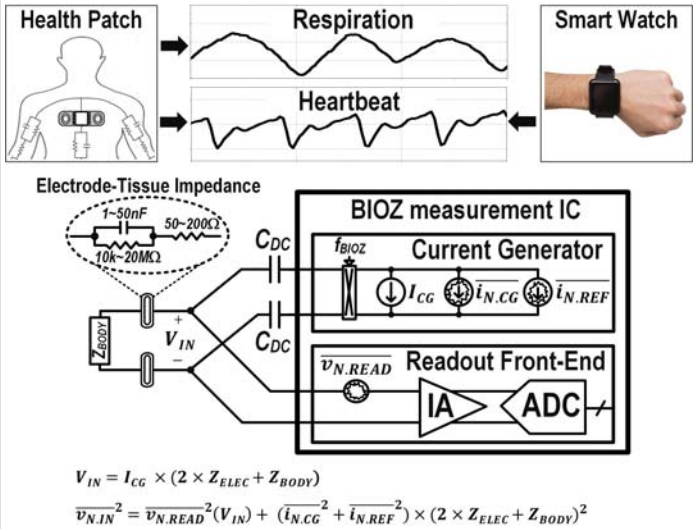

Figure 22.5.1: BIOZ measurement method via 2-electrodes and resulting input signal and input-referred noise from RFE, CG and reference.

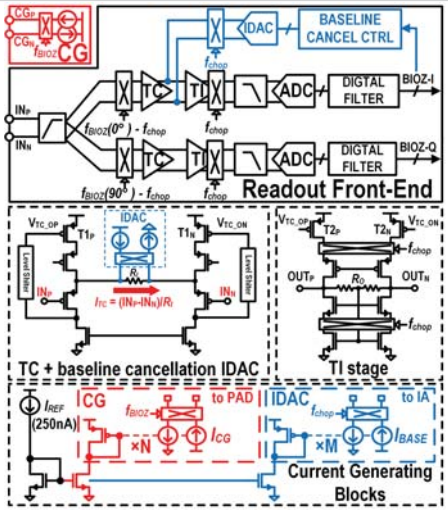

Figure 22.5.2: Top block diagram and circuit diagram of CBIA compromises TC and TI, as well as current-generating blocks (CG and IDAC) sharing a reference current.

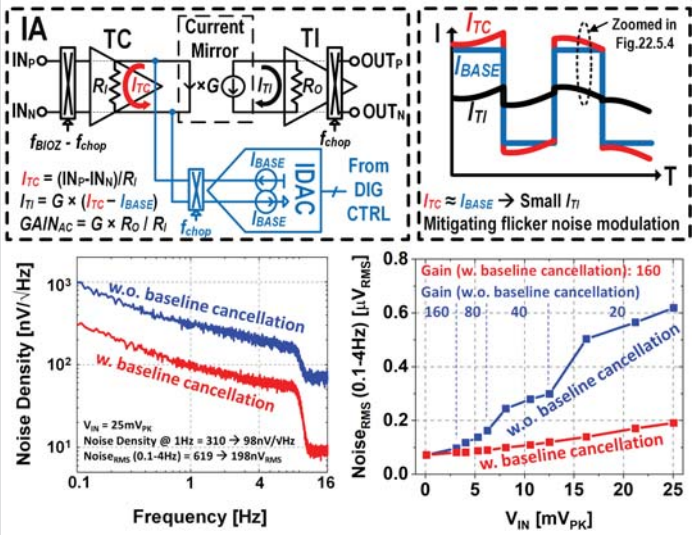

Figure 22.5.3: Operating principle of CBIA with baseline cancellation and resulting noise improvement.

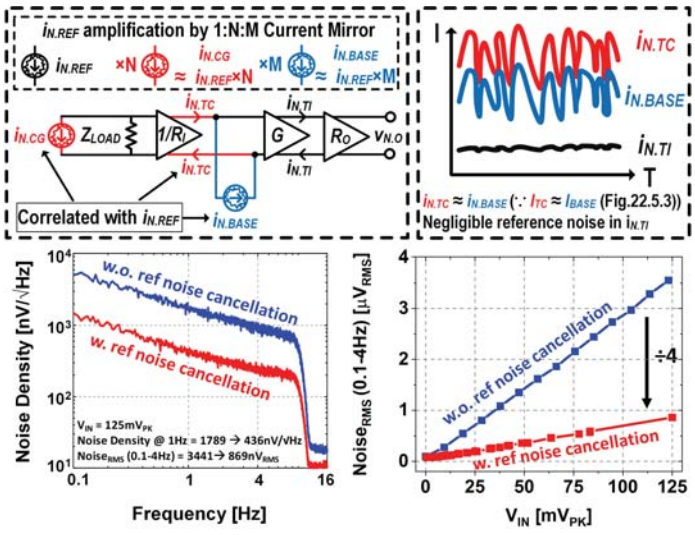

Figure 22.5.4: Correlated reference noise cancellation and resulting noise improvement.

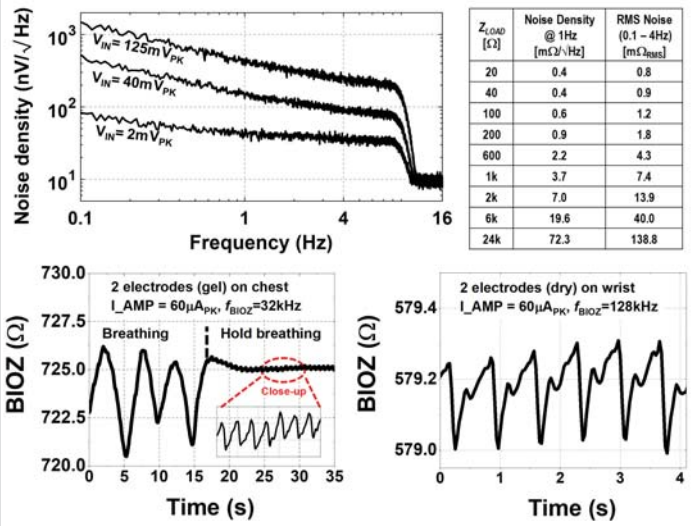

Z_{LOAD} [Ω]	Noise Density @ 1Hz [mΩ/√Hz]	RMS Noise (0.1 – 4Hz) [$mΩ_{RMS}$]
20	0.4	0.8
40	0.4	0.9
100	0.6	1.2
200	0.9	1.8
600	2.2	4.3
1k	3.7	7.4
2k	7.0	13.9
6k	19.6	40.0
24k	72.3	138.8

Figure 22.5.5: Noise and body measurement results (respiration and heartbeat) from chest and wrist of human through 2 gel and dry electrodes, respectively.

		This work	JSSC 18 [1]	VLSI 17 [2]	ISSCC 17 [3]	TCAS-II 16 [4]	MAX30001	ADS1292R
Technology (nm)		55nm	130nm	180nm	65nm	130nm	N/A	N/A
Area (mm^2)		0.74	0.96	0.88	3.2	13.8	N/A	N/A
Supply (V)		1.2	1.5/3.5	1.2/1.8	1.2	1.2	1.8	3
Stimulation signal		Square (I)	Pseudo-sine (I)	Square (I)	Pseudo-sine (I)	Square (I)	Square (I)	Square (V)
Input range (Ω)		24k	10k	1k	500[1]	623.5	5.625k[1]	10k
Current mag. (μA_{pk})		5 – 100	5 – 50	5 – 100	50 – 500	0 – 169	8 – 96	0 – 100
Current freq. (kHz)		1 – 1024	4 – 100	1 – 1024	10 – 256	0.25 – 1240	0.125 – 131	32 – 64
Noise		0.4 mΩ/√Hz (R=40Ω, 100μA_{PK}) 7.0 mΩ/√Hz (R=2kΩ, 60μA_{PK})	0.7 mΩ/√Hz (R<50Ω) 9.5 mΩ/√Hz (R=2kΩ)	1.1 mΩ/√Hz (R=20Ω) 26.0 mΩ/√Hz (R=1kΩ)	0.2 mΩ/√Hz[1,2] (R=N/A)	0.9 mΩ/√Hz[2] (R=N/A)	40m$Ω_{p-p}$ (R=680Ω)	40m$Ω_{p-p}$ (R=2kΩ)
Dynamic Range[3] (dB)		141 (BW=4Hz)	128 (BW=4Hz)	104 (BW=4Hz)	113 (BW=4Hz)	102 (BW=4Hz)	110 (BW=4Hz)	115 (BW=2Hz)
Power (μW)	Readout	18.9 – 34.9[4] / 39.1[5]	89[6]	18.7	6960	52	320	335
	CG	31.4 – 154.7	56 – 95	54 – 229		0 – 304[7]		

[1] Calculated from reported value in the paper
[2] not including CG noise
[3] $20\times\log(R_{MAX}/(2\sqrt{2}\times R_{MIN\_RMS}))$, $R_{MIN\_RMS}=R_{N.DENSITY}\times\sqrt{BW}$ or $R_{PP}/6.6$
[4] I-channel only (2 electrodes scenario), V_{IN} = 0.1 - 125mV_{PK}
[5] I- and Q-channel (4 electrodes scenario), V_{IN} = 10mV_{PK}
[6] without ADC
[7] Calculated as reported in the paper: 1.8×Injecting current

Figure 22.5.6: Comparison table with state-of-the-art BIOZ IC from academy and industry.

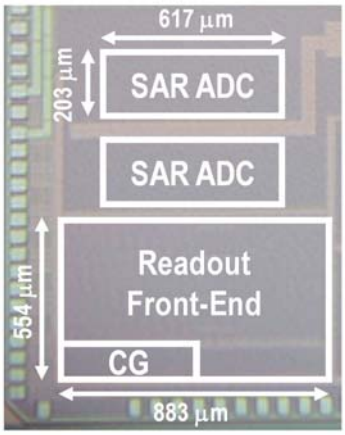

Building Block	Area [mm²]
CG	0.054
Readout Front-End	0.435
SAR ADCs	0.250
Total	0.738

Figure 22.5.7: Microphotograph and area breakdown.

978-1-5386-8531-0/19/$31.00